Research Paper

Numerical Analysis of the Transient and Non-Isothermal Channel Flow of a Third-Grade Fluid with Convective Cooling

Tiri CHINYOKA[1)*], Oluwole Daniel MAKINDE[2)]

[1)] *Center for Research in Computational and Applied Mechanics*
University of Cape Town
Rondebosch 7701, South Africa
*Corresponding Author e-mail: tchinyok@vt.edu

[2)] *Faculty of Military Science, Stellenbosch University*
South Africa

We investigate the unsteady, non-isothermal, pressure driven channel flow of a third grade liquid subject to exothermic reactions. We assume temperature dependent fluid viscosity and also that the flow is subjected to convective cooling at the channel walls. The exothermic reactions are modelled via Arrhenius kinetics and the convective heat exchange with the ambient at the channel walls follows Newton's law of cooling. The time-dependent, coupled, and nonlinear partial differential equations governing the flow and heat transfer problem are solved numerically using efficient, semi-implicit finite difference algorithms. The sensitivity of the fluid flow and heat transfer system to the various embedded parameters is explored.

Key words: unsteady channel flow; third grade fluid; variable viscosity; exothermic kinetics; convective cooling; finite difference method.

1. Introduction

The flow and material behavior of many fluids of applied engineering and industrial interest cannot be adequately described via the classical, linearly viscous, Newtonian fluid model. Examples of such fluids include: coal slurries, polymer solutions, polymer melts, drilling muds, clay coatings, elastomers, emulsions, hydrocarbon oils, grease, liquid foams, food products, etc. To this end, several alternative fluid constitutive models have been developed to characterize the inherent non-Newtonian behavior. Amongst these non-Newtonian constitutive models are those of the differential type; the so-called n-th grade fluids [1]. The first grade fluids represent the classical, linearly viscous, incompressible, and homogeneous Newtonian fluid model.

A detailed study of the general thermodynamics, stability, and uniqueness properties of fluids of the differential type (with the fluid of third grade be-

ing a special case) is presented in [2]. The third grade fluid model has been widely used to describe the non-Newtonian response of incompressible fluids [3–9]. A complete thermodynamic analysis of heat transfer problems in the flow of third grade fluids is performed in [10]. Even though a number of studies on heat and mass transfer in the flow third grade fluids have been conducted, say in [3–8, 11, 12], the thermodynamics effects that arise due to the combined effects of the Arrhenius kinetics and variable viscosity in transient Poiseuille flow have yet to be fully investigated. The current study aims to fill this gap. In particular, we employ the Frank-Kamenetskii theory [13] to model the Arrhenius exothermic reactions. In addition to the exothermic reactions in this non-isothermal flow problem, we also employ a relevant, temperature dependent, viscosity constitutive model.

Analysis of the non-linear dynamics of non-Newtonian fluids presents an interesting challenge to engineers, physicists, and mathematicians. This especially given the significance of these fluids in engineering and industrial applications as well as the serious challenges posed in experimental investigations involving such fluids. The development of accurate, robust, and efficient computational techniques for the analysis of the non-linear dynamics (as alternatives to experimental investigations) is therefore invaluable. For example, the investigations in [14] explore computational methodologies to conduct important comparative studies of the thermal loading capacities of Newtonian and viscoelastic lubricants subjected to exothermic reactions. The present study implements similarly robust, efficient, and accurate computational algorithms based on semi-implicit finite difference methods. We perform the numerical analysis to investigate the combined effects of exothermic chemical kinetics and variable viscosity on the transient flow of an incompressible, reactive, third grade fluid.

2. Mathematical model

We consider the unsteady pressure driven flow of an incompressible, reactive, variable viscosity, third grade fluid between two parallel walls. The parallel walls are subjected to symmetric convective heat exchange with the ambient. We choose the $\bar{x}$-axis parallel to the flow and the $\bar{y}$-axis normal to it, as shown in Fig. 1.
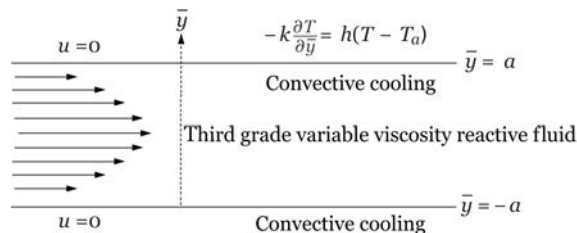

Fig. 1. Geometry of the problem.

We assume laminar, unidirectional flow in the $\bar{x}$-direction with axial velocity field $u = u(\bar{y}, \bar{t})$, transverse velocity $v = 0$, and temperature field $T = T(\bar{y}, \bar{t})$. As given in, say, [5] the governing equations for the momentum and energy balance, after appropriate modifications, can be written respectively as,

$$(2.1) \qquad \rho \frac{\partial u}{\partial \bar{t}} = -\frac{\partial \overline{P}}{\partial \bar{x}} + \frac{\partial}{\partial \bar{y}} \left[\bar{\mu}(T) \frac{\partial u}{\partial \bar{y}} \right] + \alpha_1 \frac{\partial^3 u}{\partial \bar{y}^2 \partial \bar{t}} + 6\beta_3 \frac{\partial^2 u}{\partial \bar{y}^2} \left(\frac{\partial u}{\partial \bar{y}} \right)^2,$$

$$(2.2) \quad \rho\, c_p \frac{\partial T}{\partial \bar{t}} = k \frac{\partial^2 T}{\partial \bar{y}^2} + \left(\frac{\partial u}{\partial \bar{y}} \right)^2 \left(\bar{\mu}(T) + 2\beta_3 \left(\frac{\partial u}{\partial \bar{y}} \right)^2 \right) + QC_0 A \left(\frac{KT}{\nu l} \right)^m e^{-\frac{E}{RT}}.$$

Given the geometric symmetry, we consider only the upper-half of the channel, $0 \leq \bar{y} \leq a$, and hence the relevant initial and boundary conditions are,

$$(2.3) \qquad u(\bar{y}, 0) = 0, \qquad\qquad T(\bar{y}, 0) = T_0,$$

$$(2.4) \qquad \frac{\partial u}{\partial \bar{y}}(0, \bar{t}) = 0, \qquad \frac{\partial T}{\partial \bar{y}}(0, \bar{t}) = 0, \qquad \text{for } \bar{t} > 0,$$

$$(2.5) \qquad u(a, \bar{t}) = 0, \qquad -k \frac{\partial T}{\partial \bar{y}}(a, \bar{t}) = h[T(a, \bar{t}) - T_a], \qquad \text{for } \bar{t} > 0.$$

The chemical kinetics term, governing the exothermic reactions, in the energy equation is due to [13]. Here $u = u(\bar{y}, \bar{t})$ is the fluid axial velocity, $T = T(\bar{y}, \bar{t})$ is the fluid temperature, T_a is the ambient temperature, T_0 is the fluid initial temperature, $\overline{P}$ is the modified pressure, $\bar{t}$ is the time, ρ is the fluid density, k is the thermal conductivity coefficient, c_p is the specific heat at constant pressure, h is the heat transfer coefficient, Q is the heat of reaction, A is the rate constant, E is the activation energy, R is the universal gas constant, C_0 is the initial concentration of the reacting species, a is the channel half width, l is Planck's number, K is Boltzmann's constant, ν is the vibration frequency, the normal stress modulus α_1 is a measure of the fluid viscoelasticity, the material modulus β_3 represents shear dependent viscosity, m is a numerical constant such that $m \in \{-2, 0, 0.5\}$, refer to [5] and references therein. The three values taken by the parameter m represent the numerical exponent for sensitized, Arrhenius, and bimolecular kinetics respectively [5] and references therein. As shown in Eq. (2.3), we employ zero initial condition for the fluid velocity and temperature profile. The temperature dependent viscosity, $\bar{\mu} = \bar{\mu}(T)$, follows a Nahme-type law,

$$(2.6) \qquad\qquad\qquad \bar{\mu}(T) = \mu_0 e^{-b(T - T_0)},$$

where b is a viscosity variation parameter and μ_0 is the reference viscosity at temperature T_0. We introduce the dimensionless variables and parameters, Eq. (2.7) into Eqs (2.1) and (2.2),

$$t = \frac{\overline{t}\mu_0}{\rho a^2}, \qquad x = \frac{\overline{x}}{a}, \qquad y = \frac{\overline{y}}{a},$$

$$W = \frac{u\rho a}{\mu_0}, \qquad \Theta = \frac{E(T - T_0)}{RT_0^2}, \qquad \Theta_a = \frac{E(T_a - T_0)}{RT_0^2},$$

(2.7)

$$P = \frac{\overline{P}\rho a^2}{\mu_0^2}, \qquad G = -\frac{\partial \overline{P}}{\partial x}, \qquad \mu = \frac{\overline{\mu}}{\mu_0},$$

$$\alpha = \frac{bRT_0^2}{E}, \qquad \gamma = \frac{\beta_3 \mu_0}{\rho^2 a^4}, \qquad \delta = \frac{\alpha_1}{\rho a^2},$$

$$\varepsilon = \frac{RT_0}{E}, \qquad \mathrm{Bi} = \frac{ah}{k}, \qquad \mathrm{Pr} = \frac{\mu_0 c_p}{k},$$

$$\lambda = \left(\frac{KT_0}{\nu l}\right)^m \frac{QAC_0 E a^2}{kRT_0^2} e^{-\frac{E}{RT_0}}, \qquad \Omega = \frac{\mu_0^3 E}{kR\rho^2 a^2 T_0^2},$$

and obtain the non-dimensional governing system given as Eqs (2.8) and (2.9),

(2.8) $\quad \dfrac{\partial W}{\partial t} = G + e^{-\alpha\Theta}\dfrac{\partial^2 W}{\partial y^2} - \alpha e^{-\alpha\Theta}\dfrac{\partial\Theta}{\partial y}\dfrac{\partial W}{\partial y} + \delta\dfrac{\partial^3 W}{\partial y^2 \partial t} + 6\gamma\dfrac{\partial^2 W}{\partial y^2}\left(\dfrac{\partial W}{\partial y}\right)^2,$

(2.9) $\quad \mathrm{Pr}\,\dfrac{\partial\Theta}{\partial t} = \dfrac{\partial^2\Theta}{\partial y^2} + \Omega\left(\dfrac{\partial W}{\partial y}\right)^2\left(e^{-\alpha\Theta} + 2\gamma\left(\dfrac{\partial W}{\partial y}\right)^2\right) + \lambda(1 + \varepsilon\Theta)^m e^{\frac{\Theta}{1+\varepsilon\Theta}},$

where λ, Pr, Bi, ε, δ, γ, G, α, Ω, Θ_a, respectively, represent the Frank-Kamenetskii parameter, the Prandtl number, the Biot number, activation energy parameter, material parameter, the non-Newtonian parameter, the pressure gradient parameter, the variable viscosity parameter, the viscous heating parameter, and the ambient temperature parameter.

The corresponding, non-dimensional, initial and boundary conditions are:

(2.10) $\quad W(y, 0) = 0, \qquad \Theta(y, 0) = 0,$

(2.11) $\quad \dfrac{\partial W}{\partial y}(0, t) = 0, \qquad \dfrac{\partial\Theta}{\partial y}(0, t) = 0, \qquad \text{for } t > 0,$

(2.12) $\quad W(1, t) = 0, \qquad \dfrac{\partial\Theta}{\partial y}(1, t) = -\mathrm{Bi}\left[\Theta(1, t) - \Theta_a\right], \qquad \text{for } t > 0.$

In engineering calculations, the wall shear rate (skin friction) and the wall heat transfer rate are usually the preferred measure for flow velocity (W) and temperature (Θ), respectively. In dimensionless terms, the skin friction (C_f) and the wall heat transfer rate (Nu) are,

(2.13)
$$C_f = -\frac{dW}{dy}(1,t), \qquad Nu = -\frac{d\Theta}{dy}(1,t).$$

In the following section, the Eqs (2.8) and (2.9) are solved numerically, subject to the initial conditions (2.10) and boundary conditions (2.11), (2.12) using semi-implicit finite difference algorithms.

3. Numerical algorithms

Our computational algorithms are built on the ideas from [15]. As in [14, 16], we extend the algorithm to the non-isothermal regime. Being semi-implicit finite difference methods, it is imperative to choose the implicit terms carefully and in line with numerical stability considerations. For versatility, we also take the implicit terms at the intermediate time level $(N+\xi)$ where $0 \leq \xi \leq 1$. The algorithm employed in [14] uses $\xi = 1/2$ which improves accuracy in time to second order. For pragmatic reasons, we however follow the formulation in [15] and thus take $\xi = 1$ so that we can use larger time steps and converge to steady states much faster. Indeed, with $\xi = 1$ we are free to use very large time-steps such as $\Delta t = 1$ in this article. This enables fast computations and rapid convergence to steady states and hence greatly reduces computational costs. We do not explore $\xi = 1/2$ in this study since this, in turn, would require very small time steps and high computational costs.

The finite-difference discretization of the governing equations is based on a uniform mesh and grid ($\Delta y = $ constant, $\Delta t = $ constant). We approximate both the second and first spatial derivatives with second-order central differences. The equations corresponding to the first and last mesh points are modified to incorporate the boundary conditions. The semi-implicit scheme for the velocity component reads,

(3.1)
$$\frac{\partial}{\partial t}\left(W - \delta\frac{\partial^2 W}{\partial y^2}\right) = G + e^{-\alpha\Theta^{(N)}}\frac{\partial^2}{\partial y^2}W^{(N+\xi)}$$
$$- \left[\alpha e^{-\alpha\Theta}\frac{\partial\Theta}{\partial y}\frac{\partial W}{\partial y} + 6\gamma\frac{\partial^2 W}{\partial y^2}\left(\frac{\partial W}{\partial y}\right)^2\right]^{(N)}.$$

In Eq. (3.1), and throughout this numerical section, it is understood that $\partial\#/\partial t := (\#^{(N+1)} - \#^{(N)})/\Delta t$. The equation for velocity at the next time step, $W^{(N+1)}$, then becomes,

(3.2)
$$-r_1 W_{j-1}^{(N+1)} + (1 + 2r_1) W_j^{(N+1)} - r_1 W_{j+1}^{(N+1)} = \text{ explicit terms,}$$

where $r_1 = (\xi\,\Delta t\,\mu^{(N)} - \delta)/(\Delta y^2)$ and $\mu^{(N)} = \exp(-\alpha\Theta^{(N)})$. The solution procedure for $W^{(N+1)}$ thus reduces to inversion of tri-diagonal matrices. This is

a clear advantage over a full implicit scheme which would have, among other complexities, led to unstructured matrices. The semi-implicit finite difference scheme for the temperature equation is similarly obtained. In particular, and in view of numerical stability considerations, unmixed second partial derivatives of the temperature are treated implicitly,

$$(3.3) \quad \Pr \frac{\partial \Theta}{\partial t} = \frac{\partial^2}{\partial y^2} \Theta^{(N+\xi)}$$

$$+ \left[\lambda(1 + \varepsilon\Theta)^m e^{\frac{\Theta}{1+\varepsilon\Theta}} + \Omega \left(\frac{\partial W}{\partial y} \right)^2 \left(e^{-\alpha\Theta} + 2\gamma \left(\frac{\partial W}{\partial y} \right)^2 \right) \right]^{(N)}.$$

The equation for $\Theta^{(N+1)}$ thus becomes,

$$(3.4) \qquad -r\,\Theta_{j-1}^{(N+1)} + (\Pr + 2r)\,\Theta_j^{(N+1)} - r\,\Theta_{j+1}^{(N+1)} = \text{ explicit terms,}$$

where $r = \xi\,\Delta t/\Delta y^2$. The solution procedure again reduces to inversion of tri-diagonal matrices. The schemes ((3.2) and (3.4)) were checked for consistency. For $\xi = 1$, these are first-order accurate in time but second order in space. The schemes in [14] have $\xi = 1/2$ which improves the accuracy in time to second order. As already mentioned, we use $\xi = 1$ here so that we are free to choose larger time steps and still converge to the correct steady solutions. The steady state computational results of the following section are obtained near the time $t = 100$. To reach such a high time via the extremely low time steps that would be necessary with the choice $\xi = 1/2$, would be at the expense of huge computational costs. Using the choice $\xi = 1$, on the other hand, greatly reduces computational costs as we can choose time steps as high as $\Delta t = 1$. The time step choices $\Delta t = 0.001$ and $\Delta t = 0.01$ used in the next section still gave results in real time, roughly 23 seconds and 2.3 seconds respectively to run the numerical code to time $t = 100$!

4. Results and discussion

Unless the context dictates otherwise, we employ the default parameter values, $G = 1$, $\Pr = 10$, $\Theta_a = 0.1$, $\delta = 0.0001$, $\lambda = 0.1$, $\text{Bi} = 1$, $m = 0.5$, $\varepsilon = 0.1$, $L = 1$, $\alpha = 0.1$, $\Omega = 0.1$, $\gamma = 0.1$, $\Delta y = 0.02$, $\Delta t = 0.001$, and $t = 100$.

4.1. Transient and steady flow profiles

We display, in Fig. 2, the time evolution of solutions from the transient to the steady states. The figures show a transient increase in both fluid velocity and temperature until the respective steady states are reached.
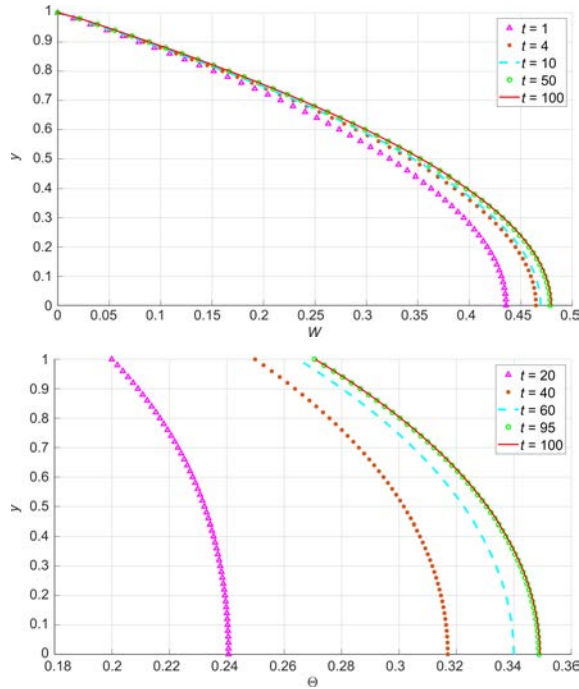
Fig. 2. Transient and steady state velocity and temperature profiles.

4.1.1. Blow up of solutions. Given the presence of exothermic reactions, it should therefore be pointed out that the steady profiles, such as those shown in Fig. 2, may not be attainable for certain values of the exothermic parameters. In particular, the reaction parameter, λ, will need to be carefully controlled as "large" values can easily lead to blow up of solutions as illustrated in Fig. 3.
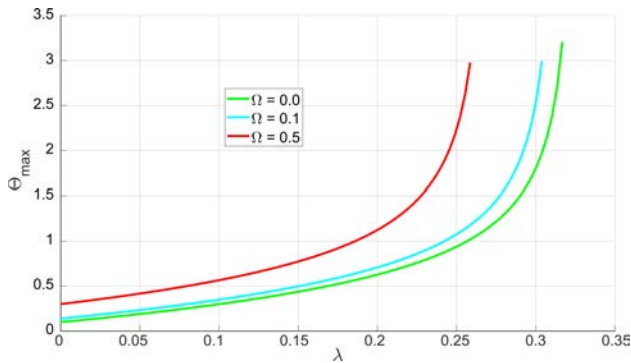

Fig. 3. Blow up of fluid temperature for large λ.

In Fig. 3, the viscous heating parameter, Ω, is included to illustrate that blow-up of solutions is intrinsically linked to the reaction parameter, λ. Even though

the viscous heating source terms are indeed also responsible for temperature increases within the fluid system, if the exothermic reactions are absent from the system, then no blow-up (thermal runaway) of solutions would occur. Viscous heating therefore only serves to either delay thermal runaway (when $\Omega \approx 0$) or speed it up (when Ω is 'large'). To conclusively illustrate this point, Fig. 4 shows that, in the absence of exothermic reactions (i.e. $\lambda = 0$) no thermal runaway is observed.
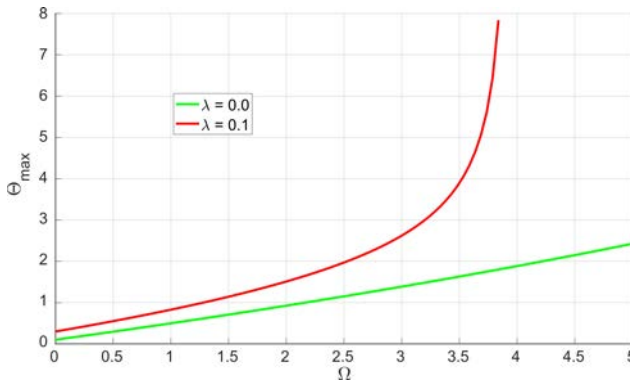
Fig. 4. Illustration that blow up of fluid temperature is related to λ.

4.1.2. Parameter dependence of solutions. In addition to the influence of the heat source terms, λ and Ω, on thermal runaway, we now also explore the sensitivity of the solutions more generally to changes in the values of the embedded parameters. The response of the velocity and temperature to varying values of the non-Newtonian parameter (γ) is illustrated in Fig. 5.

An increase in the parameter γ effectively leads to corresponding increases in those non-Newtonian properties of the fluid linked to increased resistance to flow as well as to reduced strength of the heat source terms. This respectively explains the reduction in both the fluid velocity and fluid temperature with increasing non-Newtonian character as measured by the parameter γ, see Fig. 5. The influence of the variable viscosity parameter on the velocity and temperature profiles is shown in Fig. 6.

Increasing the parameter α reduces the fluid viscosity and hence also reduces the fluid's resistance to flow. This leads to increased fluid velocity as illustrated in Fig. 6. The increased velocity, and hence also increased shear rates ($|\,dW/\,dy|$), in turn increase the viscous heating source terms in the temperature equation and hence also increase the fluid temperature as shown in Fig. 6. The effects of the chemical kinetics exponent m on the velocity and temperature profiles are shown in Fig. 7.
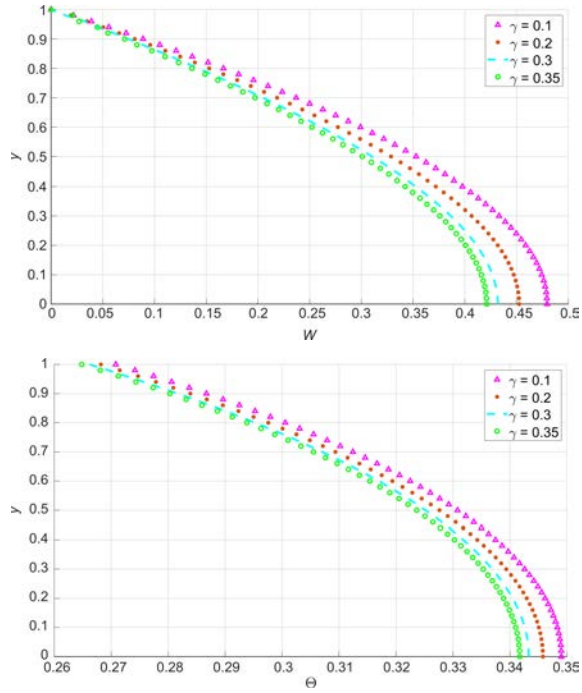
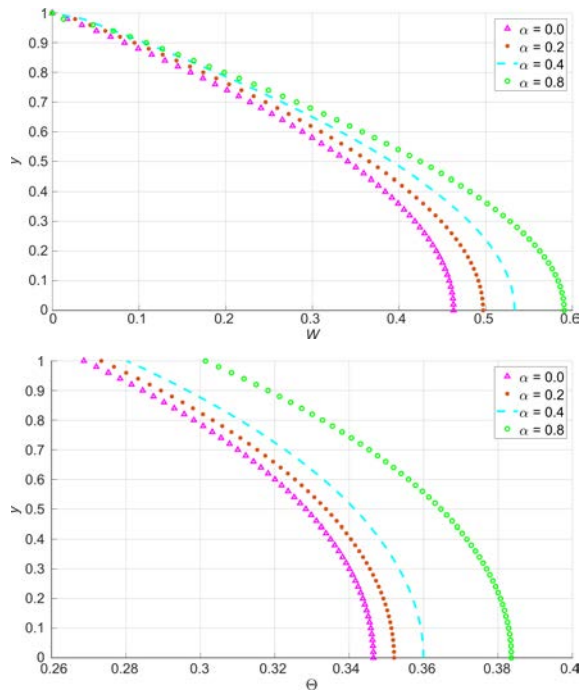FIG. 5. Effects of non-Newtonian parameter (γ) on velocity and temperature.

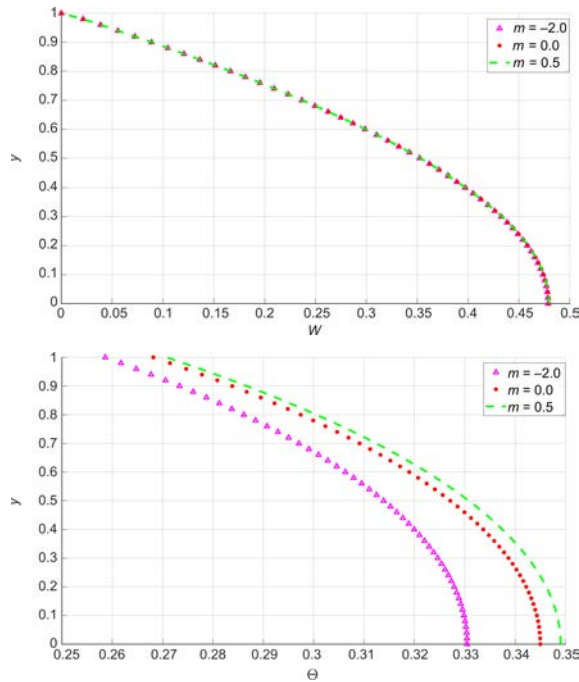FIG. 6. Effects of variable viscosity parameter (α) on velocity and temperature.

FIG. 7. Effects of parameter (m) on velocity and temperature.

Figure 7 shows that the internal heat generated in the fluid during a bi-molecular type of exothermic chemical reaction ($m = 0.5$) is higher than that generated either under the Arrhenius ($m = 0$) or sensitized ($m = -2$) reaction types. This is expected given the relationship between the parameter m and Arrhenius source terms in the temperature equation. Since the parameter m only enters the velocity equation implicitly through the temperature/viscosity coupling, the effects of m on the fluid velocity are not as pronounced. The effects of the activation energy parameter ε on the velocity and temperature profiles are shown in Fig. 8. The parameter ε plays a more-or-less similar role (both mathematically and physically) to the parameter m described in Fig. 7 and hence its effects are similarly explained.

The effects of the Biot number Bi on the velocity and temperature profiles are illustrated in Fig. 9.

As seen from the temperature boundary condition (2.12), higher Biot numbers correspond to higher degrees of convective cooling at the channel walls leading to lower temperatures at these walls and hence also in the bulk fluid. The overall fluid temperature thus decreases with increasing the Biot number as the bulk fluid continually adjusts to the lower wall temperatures, see Fig. 9. The reduced temperatures correspondingly decrease the fluid viscosity and hence also marginally decreases the fluid velocity due to flow resistance. The effects of the
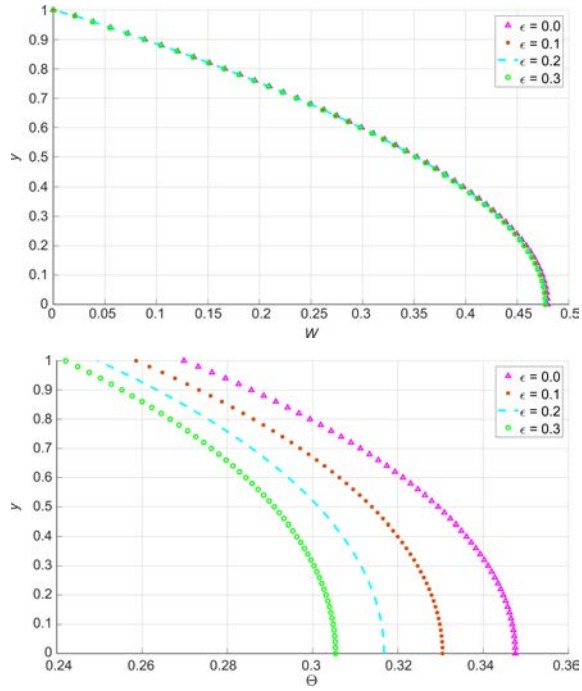
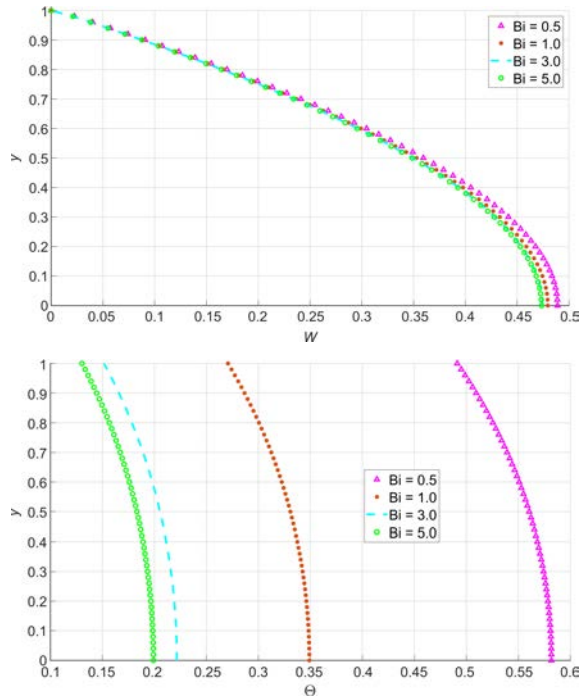FIG. 8. Effects of activation energy parameter (ε) on velocity and temperature.

FIG. 9. Effects of the Biot number (Bi) on velocity and temperature.

Prandtl number Pr on the velocity and temperature profiles are illustrated in
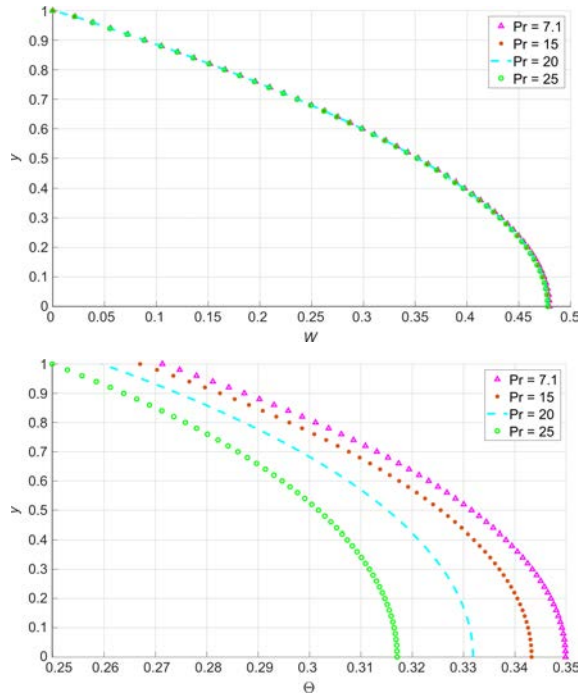Fig. 10.

Fig. 10. Effects of the Prandtl number (Pr) on velocity and temperature.

Larger values of the Prandtl number correspondingly decrease the strength
of the source terms in the temperature equation and hence in turn reduces the
overall fluid temperature as clearly illustrated in Fig. 10. As already pointed
out, the reduced fluid temperature decreases the fluid viscosity and hence re-
duces fluid velocity. The effects of the reaction parameter λ on the velocity and
temperature profiles are illustrated in Fig. 11.

The reaction parameter λ plays a roughly opposite role to the Prandtl number
just described. Increased values of λ lead to a significant increase in the exother-
mic reaction strength and hence significantly increase the fluid temperature as
shown in Fig. 10 and also in the blow up, Fig. 3. The significant temperature rise
leads to equally significant reductions in the fluid viscosity hence significantly
also increasing the fluid velocity. The effects of the viscous heating parameter Ω
on the velocity and temperature profiles are illustrated in Fig. 12. The effects of
Ω mirror those of λ.

The dependence of the skin friction, C_f, on the reaction parameter, λ, is
illustrated in Fig. 13 for various values of the viscosity variation parameter α.
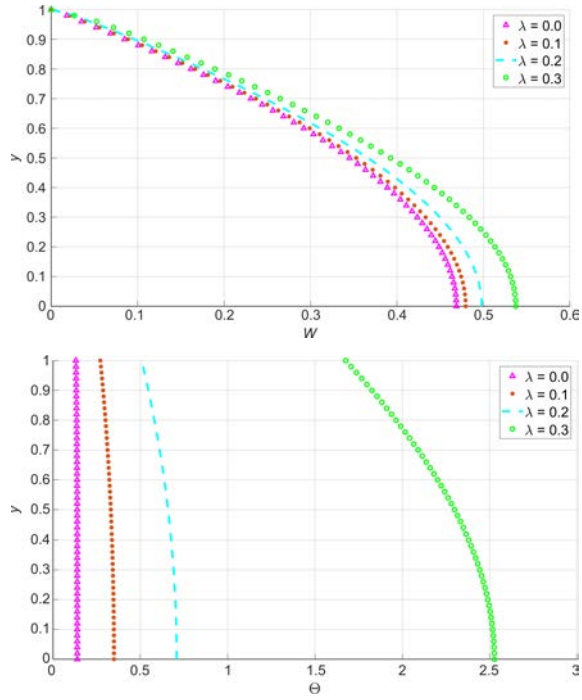Similarly, Fig. 14 shows the dependence of the skin friction on λ for various

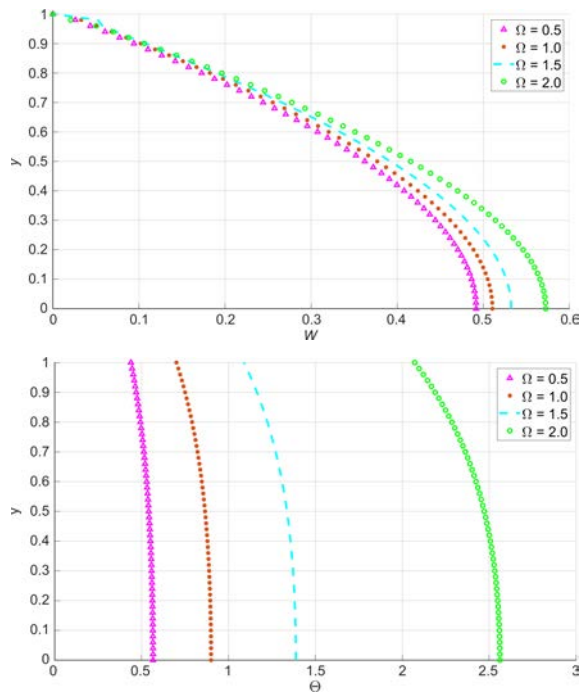FIG. 11. Effects of the reaction parameter (λ) on velocity and temperature.

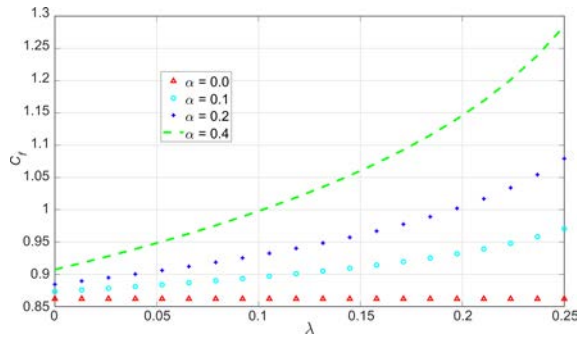FIG. 12. Effects of the viscous heating parameter (Ω) on velocity and temperature.
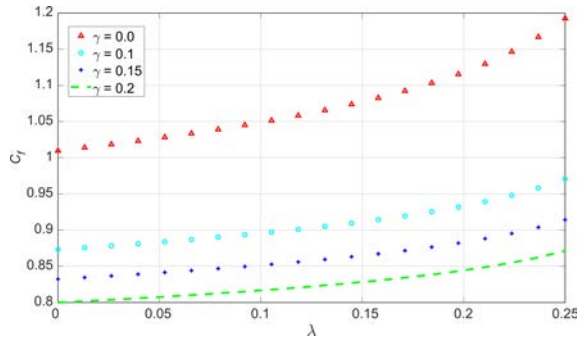
FIG. 13. Variation of wall shear stress with λ and α.

FIG. 14. Variation of wall shear stress with λ and γ.

values of the non-Newtonian parameter γ. In general, parameters that decrease (respectively increase) the fluid velocity correspondingly decrease (respectively increase) the skin friction.

The dependence of the wall heat transfer rate on λ is illustrated in Fig. 15 for various values of α. Similarly, Fig. 16 shows the dependence of the wall heat transfer on λ for various values of γ. As with the wall shear stress, parameters
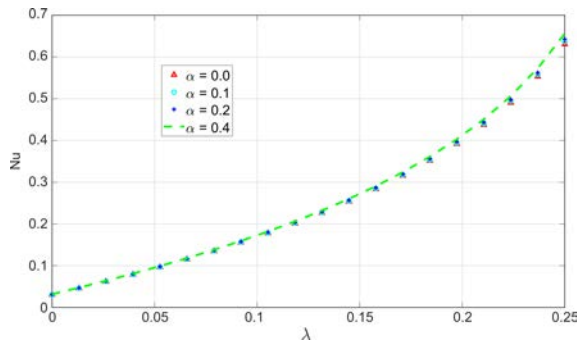

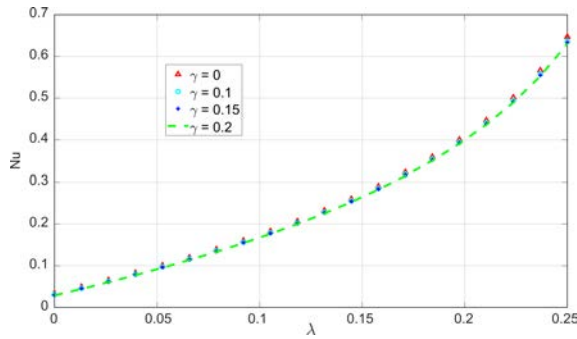FIG. 15. Variation of wall heat transfer rate with λ and α.

Fig. 16. Variation of wall heat transfer rate with λ and γ.

that decrease (respectively increase) the fluid temperature will correspondingly decrease (respectively increase) the wall heat transfer. Figures 13–16 were obtained at time $t = 100$ but using the larger time-step, $\Delta t = 0.01$.

5. CONCLUSION

We employ robust and efficient finite difference algorithms to investigate the transient and steady state characteristics in the non-isothermal, pressure driven channel flow of a reactive variable viscosity third-grade liquid subjected to convective cooling at the channel walls. We observe that, for low values of reaction parameters, there is a transient increase in both fluid velocity and temperature until steady states are reached. We also observe that, at steady state, there is an increase in both fluid velocity and fluid temperature with an increase in the reaction strength; viscous heating; and viscosity variation parameter. A decrease (at steady state) in both fluid velocity and fluid temperature is observed with an increase in the non-Newtonian character. The possible finite time blow-up of solutions means that the reaction strength needs to be carefully controlled. We also notice that due to the nature of especially the viscosity coupling, the fluid velocity and fluid temperature either both increase or both decrease. Parameters that increase the viscosity would decrease these two flow quantities and similarly those that decrease the viscosity would increase the two flow quantities. The behaviour of the skin friction and the wall heat transfer rate respectively mirror the corresponding behaviour of the fluid velocity and the fluid temperature.

REFERENCES

1. TRUESDELL C., NOLL W., *The non-linear field theories of mechanics*, Vol. 111/3: *Handbuch der Physik/Encyclopedia of Physics*, S. Flügge [Ed.], Springer, Berlin 1965, doi: 10.1007/978-3-642-46015-9.

2. RAJAGOPAL K.R., *On boundary conditions for fluids of the differential type: Navier-Stokes equations and related non-linear problems*, Plenum Press, New York 1995, doi: 10.1007/978-1-4899-1415-6_22.

3. SALAWU S.O., OKE S.I., Inherent irreversibility of exothermic chemical reactive third-grade Poiseuille flow of a variable viscosity with convective cooling, *Journal of Applied and Computational Mechanics*, **4**(3): 167–174, 2018, doi: 10.22055/jacm.2017.22933.1144.

4. ADESANYA S.O., FALADE J.A., JANGILI S., ANWAR BÉG O., Irreversibility analysis for reactive third-grade fluid flow and heat transfer with convective wall cooling, *Alexandria Engineering Journal*, **56**(1): 153–160, 2017, doi: 10.1016/j.aej.2016.09.017.

5. CHINYOKA T., MAKINDE O.D., Buoyancy effects on unsteady mhd flow of a reactive third-grade fluid with asymmetric convective cooling, *Journal of Applied Fluid Mechanics*, **8**(4): 931–941, 2015, https://www.sid.ir/en/journal/ViewPaper.aspx?id=464575.

6. CHINYOKA T., MAKINDE O.D., Unsteady hydromagnetic flow of a reactive variable viscosity third-grade fluid in a channel with convective cooling, *International Journal for Numerical Methods in Fluids*, **69**: 353–365, 2012, doi: 10.1002/fld.2562.

7. MAKINDE O.D., CHINYOKA T., Numerical study of unsteady hydromagnetic generalized Couette flow of a reactive third-grade fluid with asymmetric convective cooling, *Computers & Mathematics with Applications*, **61**(4): 1167–1179, 2011, doi: 10.1016/j.camwa.2010.12.066.

8. CHINYOKA T., MAKINDE O.D., Analysis of transient generalized Couette flow of a reactive variable viscosity third-grade liquid with asymmetric convective cooling, *Mathematical and Computer Modelling*, **54**(1–2): 160–174, 2011, doi: 10.1016/j.mcm.2011.01.047.

9. SIDDIQUI A.M., MAHMOOD R., GHORI Q.K., Thin film flow of a third grade fluid on a moving belt by He's homotopy perturbation method, *International Jornal of Non-Linear Science Numerical Simulation*, **7**(1): 1–8, 2006, doi: 10.1515/IJNSNS.2006.7.1.7.

10. FOSDICK R.L., RAJAGOPAL K.R., Thermodynamics and stability of fluids of third grade, *Proceedings of the Royal Society of London. A: Mathematical and Physical Sciences*, **369**(1738): 351–377, 1980, doi: 10.1098/rspa.1980.0005.

11. YÜRÜSOY M., PAKDEMIRLI M., Approximate analytical solutions for the flow of a third grade fluid in a pipe, *International Journal of Non-Linear Mechanics*, **37**(2): 187–195, 2002, doi: 10.1016/S0020-7462(00)00105-0.

12. MASSOUDI M., CHRISTE I., Effects of variable viscosity and viscous dissipation on the flow of a third grade fluid in a pipe, *International Journal of Non-Linear Mechanics*, **30**(5): 687–699, 1995, doi: 10.1016/0020-7462(95)00031-I.

13. FRANK-KAMENETSKII D.A., *Diffusion and heat transfer in chemical kinetics*, Plenum Press, New York, 1969, https://trove.nla.gov.au/version/26980518.

14. CHINYOKA T., Computational dynamics of a thermally decomposable viscoelastic lubricant under shear, *ASME Journal of Fluids Engineering*, **130**(12): 121201 (7 pages), 2008, doi: 10.1115/1.2978993.

15. CHINYOKA T., RENARDY Y.Y., RENARDY M., KHISMATULLIN D.B., Two-dimensional study of drop deformation under simple shear for Oldroyd-B liquids, *Journal of Non-Newtonian Fluid Mechanics*, **130**(1): 45–56, 2005, doi: 10.1016/j.jnnfm.2005.07.005.

16. IREKA I.E., CHINYOKA T., Analysis of shear banding phenomena in non-isothermal flow of fluids governed by the diffusive Johnson-Segalman model, *Applied Mathematical Modelling*, **40**(5–6): 3843–3859, 2016, doi: 10.1016/j.apm.2015.11.005.